Effect of Parasitic Polytypes on Ballistic Electron Transport in Chemical Vapor Deposition Grown 6h-Sic Epitaxial Layers

Ilan Shalish*

Electrical and Computer Engineering, Ben Gurion University of the Negev, Beer Sheva, 8410501 Israel

*Corresponding author: E-mail: shalish@bgu.ac.il

Abstract

Growth of epitaxial layers is required for most of today's devices. Epilayer growth is commonly carried out under conditions less optimal than those of bulk growth. In materials having multiple stable polytypes, such as SiC, it may facilitate concurrent nucleation of undesired polytypes. Using ballistic electron emission spectroscopy, we have repeatedly encountered a spectral feature in chemical vapor deposition (CVD) grown 6H-SiC layers that was absent in spectra of bulk material. This feature is suggested to belong to 4H-SiC inclusions. The presence of a concurrent Schottky barrier in our CVD epilayers coincides with an observation of a lower Fermi level pinning position compared with bulk material. Copyright © VBRI Press.

Introduction

Silicon carbide represents the most mature growth and device technologies among the wide bandgap semiconductors and is a promising candidate material for high temperature and high power electronic device applications [**1, 2, 3**]. Of the large number of its possible polytypes, 4H- and 6H-SiC are commercially available in a quality considered appropriate for device applications. Doping variations, required in the utilization of many devices, are commonly achieved by epitaxial growth. The growth of epitaxial layers (epilayers) is carried out under conditions different than those of bulk growth, both thermodynamically and kinetically. Several theoretical works addressed the nucleation of polytypes from the energetic point of view [**4-5**]. Presence of undesired polytypes may alter the electrical properties of the material. In this paper, we report the effect of a parasitic polytype, possibly 4H, on the properties of CVD grown epilayers of 6H-SiC. Our results depict the electronic effect of apparently a fundamental problem in present-day CVD-grown SiC material on the transport properties of 6H-SiC and may relate to several peculiarities observed in device characteristics of this material.

Experimental details

The SiC samples used in this study were cut from wafers purchased from CREE Research. Three n-type 280-μm-thick 6H-SiC (1000) wafers were used. One wafer was cut on-axis and nitrogen doped $4 \times 10^{17}/cm^3$. The other two wafers were cut 8° off-axis with a 10-μm-thick n-type epilayer grown by CVD on their Si face. The substrates and the epilayers were nitrogen doped to levels of $\sim 1 \times 10^{18}/cm^3$ and $\sim 1 \times 10^{16}/cm^3$, respectively. The sample preparation procedure has been described elsewhere [**6**].

Ballistic electron emission spectra were obtained at *room temperature* in *air* using model AIVTB-4 scanning tunneling microscope (STM), Surface-Interface Inc., with a gold tip. Details of the scanning tunneling microscope setup and operation have been described elsewhere [**7**]. The typical tip current was 3 nA. To increase the typically low signal-to-noise ratio, we averaged $1-5 \times 10^4$ spectra to obtain the final spectrum. First derivatives were used to define the thresholds. The overall energy error is estimated to be 0.07 eV. The high-energy edge of the spectra was limited by the tip-current stability in each of the samples.

Photoluminescence was excited at room temperature using a HeCd laser (325 nm, 12 mW). The emitted luminescence was monochromatized, filtered, and sensed using a GaAs photomultiplier tube or Si CCD camera. Wavelengths were scanned in 1 nm steps from 375 to 460 nm.

Results and discussion

Fig. 1 shows ballistic electron emission spectra (BEES) obtained from the two CVD epilayer wafers. Both spectra manifest three thresholds. In epilayer A (top), the thresholds are observed at 1.22, 1.75, and 2.25 eV. In epilayer B (Bottom), the thresholds are observed at 1.27, 1.72, and 2.21 eV. The first threshold in each of the spectra represents the energy relative to the Fermi level in the metal required to introduce an electron into the conduction band minimum (CBM). This energy is equal to the Schottky barrier of the metal contact (Pt in our case) and marks the pinning position of the Fermi level relative to the CBM at the surface.
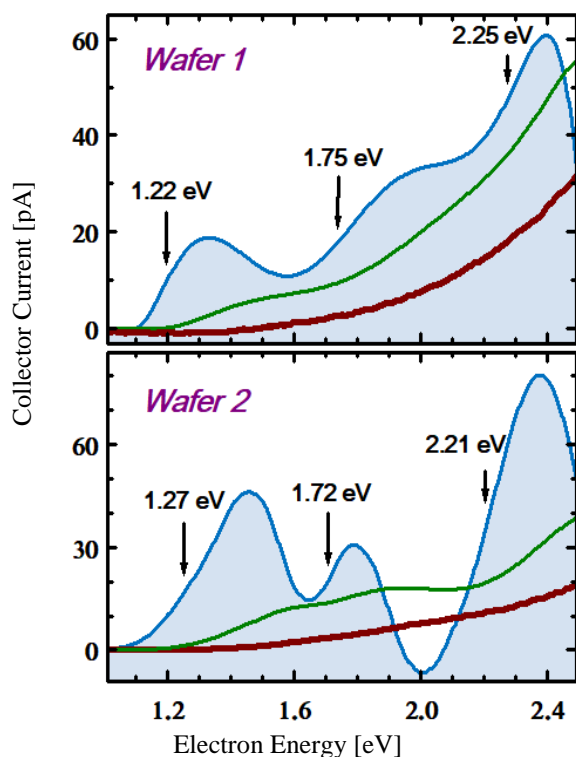

Fig. 1. (Red) Ballistic electron emission spectra obtained from two CVD-grown 6H-SiC epilayers with Pt contacts. The y-axis shows collector current. The first (green) and second (blue) derivatives are given in arbitrary units.

Fig. 2 shows a BEES spectrum obtained from the third wafer (bulk grown with no epilayer). In this case, only two thresholds are observed at 1.36 and 2.37 eV and the Fermi level pinning position is observed at a slightly higher energy compared with the CVD epilayer spectra of **Fig. 1** (1.36 vs. 1.22 and 1.27 eV respectively).

Fig. 3 presents room temperature band-edge photoluminescence spectra obtained from the 6H-SiC samples of **Fig. 1** and **Fig. 2** (with and without CVD epilayers).

A spectrum obtained under the same conditions from 4H-SiC is added for reference. In addition to the main feature at 2.93 eV, the CVD epilayer photoluminescence spectrum contains a peak at

3.19 eV, coinciding with the main feature of the 4H-SiC spectrum. This feature is absent in the spectrum of the 6H-SiC bulk sample.
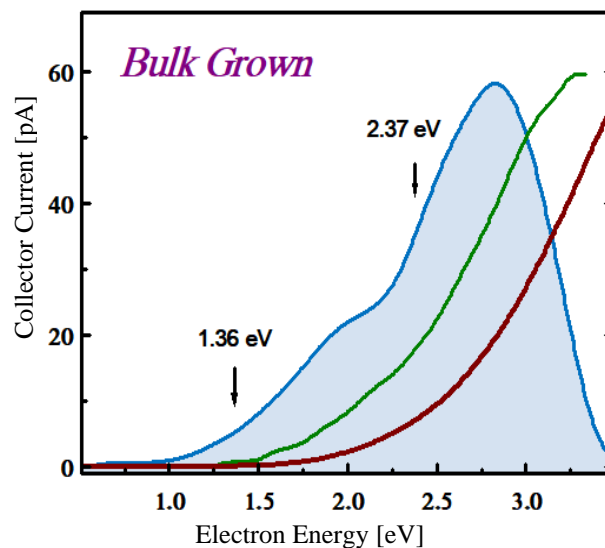

Fig. 2. (Red) Ballistic electron emission spectrum obtained from bulk-grown 6H-SiC. The y-axis units relate to the collector current. The first (green) and second (blue) derivatives are given in arbitrary units.
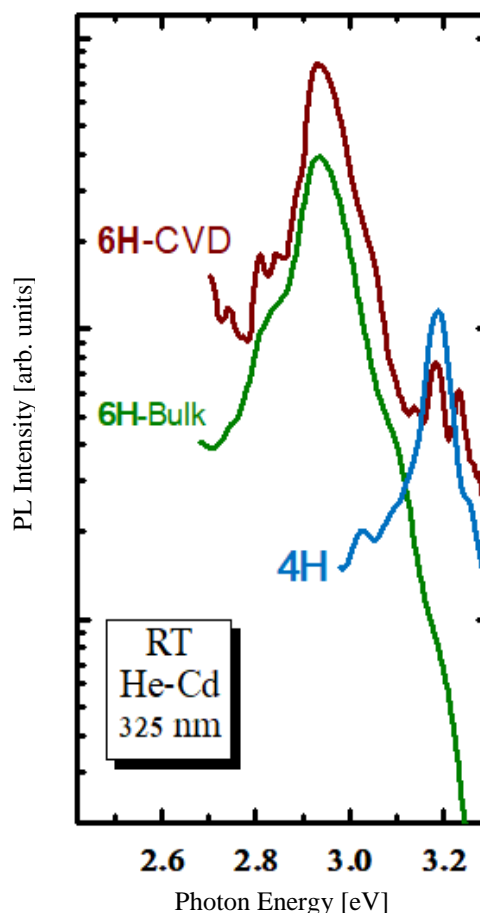

Fig. 3. Band-edge photoluminescence spectra of CVD epilayer 6H-SiC, bulk grown 6H-SiC, and reference spectrum of 4H-SiC measured under the same conditions.
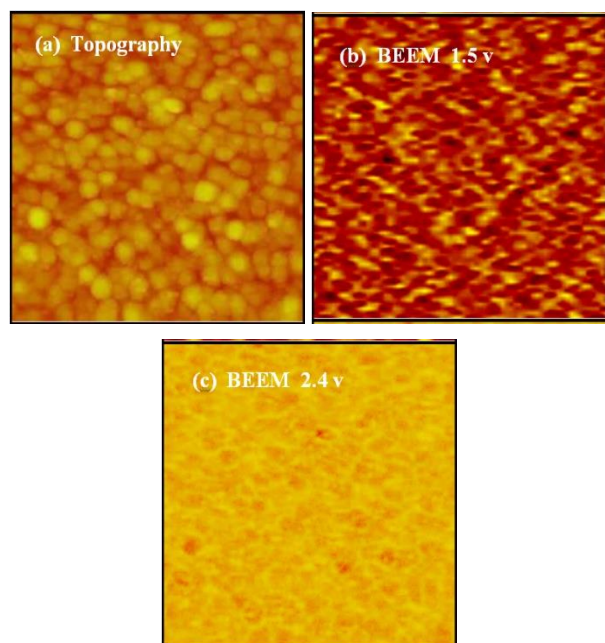
Fig. 4. Typical STM/BEEM images: (a) topography, (b) BEEM at tip voltage of 1.5 V, and (c) BEEM at tip voltage of 2.4 V.

Fig. 4 presents typical STM and ballistic electron microscopy (BEEM) images obtained from a sample cut from the first CVD epilayer wafer. **Fig. 4a** is a (2000 Å) × (2000 Å) topographic image of the Pt grains. **Fig. 4b** is a BEEM image taken at tip bias of -1.5 V, about halfway between the first two BEES thresholds observed on the CVD epilayer samples. The variations presented by the colors span a current range of less than 1 pA which is mainly a featureless noise modulating a rather smooth and featureless image. **Fig. 4c** is a BEEM image taken at tip bias of -2.4 V, well above the third BEES threshold. This BEEM image contains less noise, but the observed features reveal no more than the well-known modulation of the transport by the spherical shape of the metal grains [**8**].

To analyze these data, we refer to ab-initio calculations of the 6H-SiC conduction band. In **Fig. 5**, we plot the band structure as calculated by Wenzien *et al.* using quasiparticle corrected density functional theory in the local density approximation (DFT-LDA) [**9**]. For clarity, we show only the relevant bands. The CBM appears between the M and the L symmetry points of the first Brillouin zone. The next conduction band feature appears near the K symmetry point. In addition to this feature, a minimum of the second conduction band appears around the same energy offset right above the CBM. Both these features should be expected to contribute to the density of states at the same energy offset from the CBM, and hence cannot be distinguished by BEES. In our spectra, they appear ~1 eV above the CBM (the third threshold in the spectra of **Fig. 1** and the second in **Fig. 2**). **Table 1** compares this value with calculated values from the literature obtained with several methods. Our experimentally measured value is smaller than the

calculated values by 0.2 to 0.6 eV. This difference is partly expected as our measurements were carried out at room temperature, and may in part result from the inaccuracies of both the experiment and the calculation methods. At any event, the calculated band structure can only account for two BEES thresholds within the energy range of our measurements. Yet, in the case of CVD grown epilayers, we observe another threshold.

Table 1. Comparison of calculated energy difference between the CBM and the nearest singularity with the value observed by BEES in this work.

Source	Ref.	Method	ΔE [eV]
Limpijumnong *et al.*	10	LMTO	1.2
Wenzien *et al.*	9	DFT-LDA	1.45
Wenzien *et al.*	9	Quasiparticle	1.63
Persson and Lindefelt	11	DFT-LDA	1.41
This work			0.99±0.07

The middle threshold in the CVD spectra, at 1.72 (wafer 1) and 1.75 eV (wafer 2), is not explained by calculated band structure. Hence, it may not be associated with a band feature of 6H-SiC. Instead, it may be explained as a concurrent Schottky barrier residing in parallel with that of 6H-SiC\Pt. Coexistence of multiple Schottky barriers implies coexistence of multiple metallic phases or multiple semiconducting phases. Since only Pt was deposited and no reaction seemed to have taken place, the explanation seems to lie in the presence of another semiconductor [**12**]. This is further supported by the absence of this feature in the spectra of the bulk sample, where the preparation and measurement were identical except for the semiconductor growth.
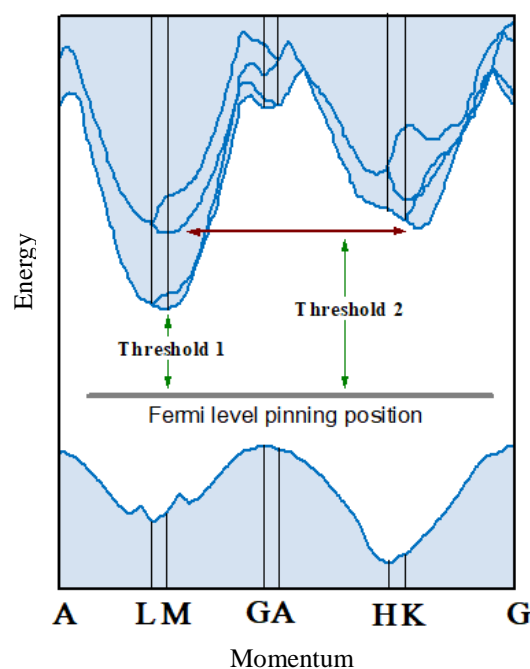

Fig. 5. Ab-initio calculated band structure of 6H-SiC (from Wenzien *et al.* [**10**]).

Parasitic polytypes in 6H-SiC are not uncommon, and commercial growers of SiC often take account of possible inclusions in their definition of high quality material. Reports in the literature have dealt mainly with inclusions of 3C-SiC [13, 14, 15] but also with 4H- and 15R-SiC [16] in CVD homoepitaxies of 6H- and 4H-SiC. Parasitic polytype inclusion in CVD homoepitaxies of 6H- and 4H-SiC have recently been studied by Okojie *et al.* and Tumakha *et al.* using low energy electron-excited nanoluminescence (LEEN) [17, 18]. The Schottky barrier of Pt on 3C-SiC is ~0.85 eV [19]. This value lies below the Schottky barrier of the 6H-SiC host, and thus cannot be detected by BEES.

The next 3C-SiC conduction band valley, where a threshold could be expected, is ~3 eV above the 3C-SiC CBM [9]. Therefore, the possible presence of 3C-SiC cannot account for any of the thresholds we observe. This suggests that BEES is practically blind to 3C-SiC inclusions in a 6H-SiC host within the studied energy range.

From the point of view of total energy of formation, the two polytypes with energies close to that of the 6H polytype are indeed 4H and 15R [4, 20]. The bandedge emission of the 15R polytype cannot be distinguished at room temperature from that of the 6H [21]. Therefore, our room temperature PL cannot exclude 15R presence. Inclusion of the 15R polytype was studied using BEES by Im *et al.* [22]. They observed three BEES thresholds: 1.28, 1.55, and 1.79 eV. While the first and the last are only slightly higher than our first and second thresholds in our CVD spectra, we do not observe their second threshold. This renders less likely an inclusion of the 15R polytype in our samples, leaving us with 4H-SiC.

Indeed, the observed 1.72-1.75 eV threshold in our CVD 6H-SiC epilayers matches a Pt Schottky barrier height (1.72 eV) observed using the same method and under the same conditions on 4H-SiC [6] Furthermore, a peak is observed in the photoluminescence spectrum of our 6H-SiC (**Fig. 3**) that matches the position of the band-edge emission peak we observed under the same conditions in 4H-SiC photoluminescence spectra. The same peak is missing in PL spectra of our bulk-grown sample. It therefore seems likely that this threshold is caused by inclusions of the 4H polytype in our CVD grown 6H-SiC epilayers. A similar luminescence feature was observed in CVD epilayers of 6H-SiC using LEEN at room temperature by Tumakha *et al.,* and as well were attributed to extrinsic bandedge luminescence from parasitic polytype inclusions [18].

Naturally, if BEES suggests inclusions, one may expect to be able to image them by BEEM. The relatively uniform BEEM images we observe suggest that the typical lateral size of the inclusions may either be larger than the largest possible scan-size in our system (6 μm), or smaller than our BEEM lateral resolution.

In the case of the large inclusions, we must explain the presence of thresholds from both polytypes. If the inclusion is thinner than the electron ballistic range in this material, both polytypes may be sensed at the same lateral position. Ballistic transport in heterostructures of this type has been investigated with BEES [23]. The inclusion may either be on top or even be buried within the ballistic range and still give rise to a BEES threshold due to coherent scattering. Electron ballistic ranges in semiconductors can vary, but may exceed a few hundreds of angstroms [23]. This scenario thus suggests an inclusion structure of wide thin plates. A similar structure of 3C-SiC inclusions in 6H- and 4H-SiC CVD homoepitaxies has been observed by transmission electron microscopy (TEM) [13, 15]. In other studies, inclusions were shown to form thin bands in CVD epilayers, which may have the same effect on ballistic electron transport [17, 18].

We have performed Monte-Carlo simulations of BEES on 6H-SiC, taking into account the modulation of ballistic current by heterostructures near the metal-semiconductor interface. The results show that it is possible to reproduce spectra that match our experimental observations using specific structures. On the other hand, thresholds due to heterostructure scattering are sensitive to the dimensions of the heterostructure layers. Since the inclusion forms without experimental controls over its thickness or depth within the host, it is not likely that the observed threshold coincidentally matches the bandstructure of the inclusion.

In the case that the inclusion size is smaller than the BEEM resolution, electron transport at the same STM tip position will be an average of transport through each polytype present. BEEM resolution is determined by the parallel component of electron momentum in the semiconductor [24, 25]. Since the relatively large 6H-SiC unit cell results in a short Brillouin zone along the (1000) direction and the CBM occurs on the zone edge, the electrons which couple to the CBM must have a large parallel momentum. Therefore, one may expect poor lateral BEEM resolution for 6H-SiC in comparison with, e.g., GaAs. The typical lateral drift at room temperature may only degrade the effective resolution over the time necessary to take a spectrum, thereby increasing the minimum inclusion size required for detection.

Finally, several studies of polytype control issues in SiC have associated the nucleation of unwanted polytypes with the presence of various types of surface defects [13, 15]. Surface defects are also known to contribute to the pinning of the Fermi level at semiconductor-metal interfaces [26]. The Schottky-Mott limit for a Pt contact on 6H-SiC is ~2.3 eV ($\Phi_m(Pt) - \chi = 5.6 - 3.3 = 2.3\ eV$, Φ_m is the metal work function, and χ is the electron affinity). The Fermi level at the metal interfaces of our CVD epilayers (1.22 eV below the CBM) is pinned further away from the Schottky Mott limit as compared to our bulk-grown material (1.36 eV). The difference in the pinning position suggests a stronger pinning at the CVD

metal interface, possibly due to defect density, which lines up with the suggested scenario of inclusions.

Conclusion

While CVD growth is prone to produce more defects than bulk growth, the exact electrical manifestation in 6H-SiC has not been as well known. This work presents two mechanisms possibly responsible for the observed deviations of the ballistic transport properties of CVD 6H-SiC epitaxial layers: effect of 4H polytype inclusions, and pinning of the surface Fermi level. Further studies to optimize the SiC growth technology are still needed in order to find the way to avoid parasitic polytyping in SiC.

References

1. Zhang Q.; Callanan R.; Das M.K.; Ryu S.H.; Agarwal A.K.; Palmour J.W. IEEE Trans. *Power Electron.* **2010**, *25*, 2889.
2. Lin L.M.; Lai P.T.; *J. Appl. Phys.* **2007**, *102*, 054515.
3. Chelnokov V.E.; Syrkin A.L.; *Mater. Sci. Eng. B,* **1997**, *46*, 248.
4. Limpijumnong S.; Lambrecht W.R.L.; *Phys. Rev. B,* **1998**, *57*, 12017.
5. Park C.H.; Cheong B. H.; Lee, K. H.; Chang K.J.; *Phys. Rev. B,* **1994**, *49*, 4485.
6. Shalish I.; Altfeder I.B.; Narayanamurti V.; *Phys. Rev. B,* **2002**, *65*, 073104.
7. Kozhevnikov M.; Narayanamurti V.; Zheng C.; Chiu Y. J.; Smith D.L.; *Phys. Rev. Lett.,* **1999**, *82*, 3677.
8. Bauer A.; Cuberes M.T.; Prietsch M.; Kaindl G.; *Phys. Rev. Lett.,* **1993**, *71*, 149.
9. Wenzien B.; Kaeckell P.; Bechstedt F.; Cappellini G.; *Phys. Rev. B,* **1995**, *52*, 10897.
10. Limpijumnong S.; Lambrecht W.R.L.; Rashkeev S.N.; Segall B.; *Phys. Rev. B,* **1999**, *59*, 12890.
11. Persson C.; Lindefelt, U.; *Phys. Rev. B,* **1996**, *54*, 10257. *J. Appl. Phys.* **1997**, *82*, 5496.
12. Another scenario may be the formation of different Schottky barriers such as in the cases of $NiSi_2$ and $CoSi_2$ on Si(111) [for review, see Tung, R.T. J. Vac. Sci. Technol. A **1989**, *7*, 598]. This scenario is, however, highly unlikely, since it appears only in epitaxially-grown lattice-matched metal-semiconductor contacts. In our case, the Pt is polycrystalline and is not lattice-matched to the SiC.
13. Powell J.A.; Larkin D.J.; *Phys. Stat. Sol. (b),* **1997**, *202*, 529.
14. Zhou W.L.; Pirouz P.; Powell J.A.; *Mater. Sci. For.,* **1998**, 264, *417*, 268.
15. Konstantinov A.O.; Hallin C.; Pecz B.; Kordina O.; Janzen E. J., *Cryst. Grow.* **1997**, *178*, 495.
16. Foti G., *Appl. Surf. Sci.* **2001**, *184*, 20.
17. Okojie R.S.; Xhang M.; Pirouz P.; Tumakha S.; Jessen G.; Brillson L.J.; *Appl. Phys. Lett.,* **2001**, *79*, 3056.
18. Tumakha S.; Brillson L.J., Jessen G.; Okojie R.S.; Lukco D.; Zhang M.; Pirouz P.; *J. Vac. Sci. Technol. B,* **2002**, *20*, 554.
19. Shenoy P.; Moki A., Baliga B.J.; Alok D.; Wongchotigul K.; Spencer M.; *Proceedings* of 1994 IEEE International Electron Device Meeting, New York, **1994**, 411.
20. Cheng C.; Heine V.; Jones I.L.; *J. Phys.: Condens. Matter,* **1990**, *2*, 5097.
21. Ikeda M.; Matsunami H.; *Phys. Stat. Sol. (a)* **1980**, *58*, 657.
22. Im H. J.; Kaczer B.; Pelz J.P.; Limpijumnong S.; Lambrecht W.R.L.; Choyke W.J.; *J. Electron. Matter.,* **1998**, *27*, 345.
23. Sajoto T.; O'Shea J.J.; Bhargava S.; Leonard D.; Chin M.A.; Narayanamurti V.; *Phys. Rev. Lett.,* **1995**, *74*, 3427.
24. Prietsch M.; *Phys. Rep.,* **1995**, *253*, 163.
25. Narayanamurti V.; Kozhevnikov M., *Phys. Rep.,* **2001**, *349*, 447.
26. Brillson L.J.; *Surf. Sci.* **1994**, *299*, 909.